

# An algorithm for reconstruction of temperature distribution on rotating cylinder surface from a thermal camera video stream

**Abstract.** The following paper presents an algorithm developed to reconstruct a full temperature distribution of a rotating cylinder's surface. The surface is constantly monitored by an IR camera that produces a stream of images. Image acquisition is triggered by a set of equidistant angles used by electronic synchronization module. Received stream is divided into sequences with equal number of frames in each and for every valid sequence the reconstruction algorithm is performed. Finally, a full temperature map for entire cylinder surface is obtained.

**Streszczenie.** W artykule przedstawiono algorytm opracowany w celu rekonstrukcji pełnego rozkładu temperatury na powierzchni obracającego się stalowego walca, nagrzewanego indukcyjnie. Źródłem danych dla algorytmu jest strumień wideo pochodzący z kamery termowizyjnej. Uwzględniona została geometria obiektu i konieczność synchronizacji wykonywanych pomiarów względem aktualnego położenia kąтового walca. Ostatecznie, z serii zsynchronizowanych pomiarów rekonstruowany jest rozkład dla całej powierzchni walca. (Algorytm rekonstrukcji rozkładu temperatury na powierzchni obracającego się walca ze strumienia video kamery termowizyjnej).

**Keywords:** image processing, thermal imaging rotating steel cylinder, synchronization.

**Słowa kluczowe:** przetwarzanie obrazów, obrazowanie termowizyjne stalowego walca, synchronizacja.

## Introduction

In the course of conducted research on the inductively heated, rotating steel cylinder's surface temperature regulation, the authors have originally used pyrometers for temperature measurement along the circumference of the cylinder. Pyrometers were placed at fixed position along the cylinder's axis [1]. Obtained point measurements provide intrinsically limited information about the current temperature of the surface. To improve the information quality, authors have added an infrared camera to the used experimental test system, which is able to measure a selected area of the surface, not only a point. A camera of choice was the FLIR A615 [2], which is able to work at acquisition speed of 200FPS in windowed mode with 640x120px resolution and 45° FOV lenses. Such parameters renders the device a valuable part of a real-time cylinder temperature control system under condition, that a proper processing of received image stream is provided.

One of the first problems that had to be solved was the need to process temperature information about the entire surface of the cylinder, rather than a cut currently observed by the camera, as shown in figure 1.



Fig.1. A cut of cylinder surface in the camera viewport (height 120px)

To solve this issue, authors have developed an algorithm for reconstructing full temperature map of the rotating steel cylinder, discussed in the following sections of this article.

## Preprocessing

Input images, obtained from IR camera are trimmed out in order to discard portions of image irrelevant for temperature control algorithms, like borders, surroundings and areas of cylinder's strongest curvature (upper and lower part) where registered temperature is affected by both insufficient resolution (larger measured area per sensor's pixel) and Lambert's cosine law. The part of the input image left, the so-called Region of Interest – ROI, is used in further processing steps. The region is manually selected, taking into account the object and a margin of a few pixels surrounding it. This allows to significantly decrease the amount of the memory occupied by images.

At this stage, dead pixels removal procedure is also performed. Dead pixel is a measure point in a sensor, which generates values that constant or varies in small range, regardless of the expected value [3] (in this case, regardless the observed temperature). The removal is done by applying a median filter on the selected dead pixels as mask with 3x3 neighborhood.



Fig.2. Hot markers illustrate outlines of the cylinder and the horizontal marker for camera roll angle correction

The pre-processing stage also refers to the size and location of the cylinder in the camera view port (calibration algorithm). For this purpose, a set of markers, made of a resistive wire, is used. They are mounted on the cylinder and its supporting structure, as shown in figure 2 For further information on this subject is contained in [4].

Finally, after calibration is done, the IR camera is switched to windowed mode to achieve a speed of 200fps at resolution of 640x120 pixels.

## Frame synchronization

Linking individual images in order to obtain full surface map is troublesome without information about angular points, at which the image was acquired.



Fig.3. Electronic synchronization module with for IR camera

This task is performed by the electronic synchronization module, developed by the authors. It uses an incremental encoder MOK40-5000-5-BZ-N able to generate 20,000 pulses per second. A prototype of this device, with an additional experimental PCB is shown in figure 3.

The designed synchronization circuit uses a Microchip microcontroller dsPIC33FJ128MC706 and communicates with a PC via USB connection (used to read the current position and velocity). Figure 4 presents the schematic of the module shown in figure 3.

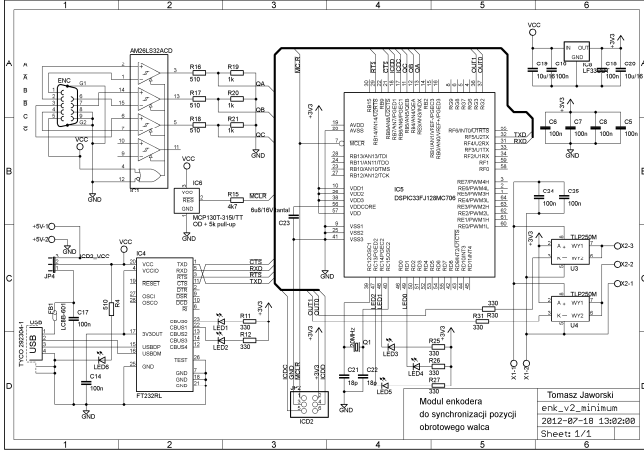


Fig.4. Synchronization module

This device generates two synchronization signals: once per cylinder's revolution cylinder and N-times per revolution. This allows the IR camera signing individual frames during the acquisition process by two bit flags when camera's input stage detects a rising edge in one of the signals. Figure 5 shows the distribution of angular synchronization points: **RS** synchronization is issued once every revolution, **IS** is the intermediate synchronization, issued N times per revolution. During the design and implementation of the algorithm,

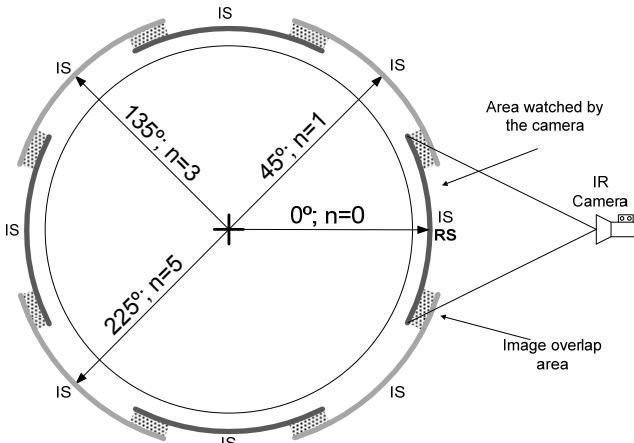


Fig.5. Image synchronization points on the circumference authors have decided to divide the surface into 8 images with one indirect synchronization pulse **IS** per image. Each image is shifted against the previous one by 45°.

Such number of areas, along with the camera viewport height provides sequence of images high enough to overlap with neighbors. Such situation is shown in figure 5 as dotted, rectangular areas.

Due to the utilization of two types of synchronization pulses, the processing software is resistant to transmission errors, occurring from time to time at camera's full speed acquisition, which requires a workstation with bandwidth at ~30MB/s connected via 1Gbps Ethernet.

Finally, the output from the developed image synchronization algorithm provides sets of images,

sequences consisting of eight consecutive frames. A sample sequence is shown in figure 7. Full sequence is then passed to final reconstruction algorithm to obtain full surface temperature map.

### Surface Reconstruction

The surface reconstruction algorithm consists of two main steps. The first one is to eliminate the influence of surface natural cylindrical curvature on the observed object. This step is carried out by the so-called *texture unwrapping* from the input image. This process can be interpreted as opposition to texturing, known from all popular 3D modeling packages. The algorithm employs a three-dimensional model of the cylinder, given by the expression (1). Its goal is to calculate a point in the three-dimensional model space coordinate system for each point of unwrapped texture, located at coordinates  $u$  and  $v$ , in texture space (two-dimensional). The model is located at the origin coordinates, denoted as  $Q(u, v) = [0 \ 0 \ 0]^T$ .

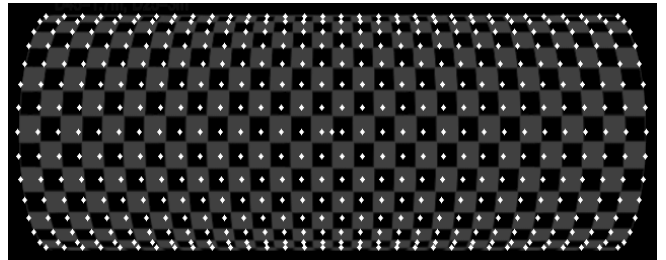


Fig.6L. A 3D model of a cylinder with a superimposed map of points

$$(1) \quad Q(u, v) = \left[ \frac{u C_L}{M_W} - \frac{1}{2} C_L; C_R \sin\left(2\pi \frac{v}{M_H}\right); C_R \cos\left(2\pi \frac{v}{M_H}\right) \right]^T$$

where  $u, v$  - coordinates of a point in the final unwrapped texture of width  $M_W$  and height  $M_H$ ,  $C_L$  - length of the cylinder,  $C_R$  - radius of the cylinder.

From all points calculated by (1) only points visible to the camera are selected. Visibility is determined on the basis of the angle between the vector  $QN(u, v)$  normal to the cylinder surface at the point  $Q(u, v)$ , given by (2), and the camera direction vector (coinciding with the optical axis)  $CD(u, v)$ , oriented on the point  $Q(u, v)$ , given by (3).

$$(2) \quad QN(u, v) = \left[ 0 \quad \sin\left(2\pi \frac{v}{M_H}\right) \quad \cos\left(2\pi \frac{v}{M_H}\right) \right]^T$$

$$(3) \quad CD(u, v) = Q(u, v) + [0 \ 0 \ D]^T$$

where:  $D$  is the distance between the camera and the cylinder geometry center.

Finally, the visibility of the surface point is determined by the scalar product sign of (2) and (3). If the condition (4) is met (which means angles between 90° and 270°), the point is considered to be visible.

$$(4) \quad QN(u, v) \cdot CD(u, v) < 0$$

Each visible point  $Q(u, v)$  is then mapped to the input image (from a thermal camera) by perspective [5] projection (5).

$$(5) \quad P^{input}(u, v) = \left[ \frac{f Q_X(u, v)}{f + Q_Z(u, v)} \quad \frac{f Q_Y(u, v)}{f + Q_Z(u, v)} \right]$$

where:  $P^{input}$  - coordinates in the input image,  $f$  - camera focal length, subscripts  $X, Y$  and  $Z$  are components of the vector  $Q(u, v)$  given by (1).

Figure 6L shows a sample visualization of the model given by (1) with only visible points  $Q(u, v)$  marked. Each of them has a corresponding  $P^{input}$  point. A result of the unwrapping algorithm, performed for a synthetic input

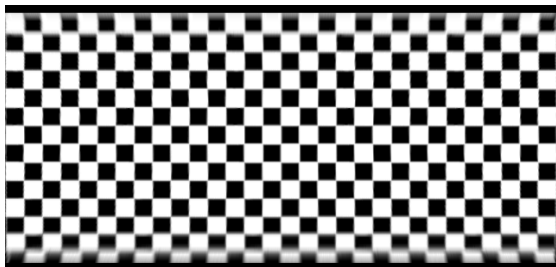


Fig.6R. Texture unwrapped by applying the 3D model image is depicted in figure 6R.

To determine the final value of each point in unwrapped texture, a bilinear interpolation was employed.

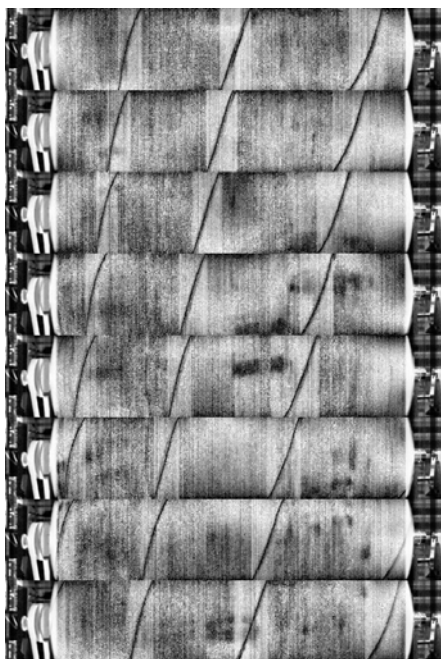


Fig.7L. A sequence of 8 images input sequence arranged from oldest to youngest

Figure 7R shows a result of unwrapping algorithm performed for an arbitrarily selected sequence of eight input images (figure 7L). To better illustrate the effectiveness of the developed algorithm, the presented images show additional marker wrapped around the cylinder (the black line). For the sake of marker visibility, all images were enhanced by individual normalization of each column, since the overall normalization rendered the marker very difficult to see.

At the moment when a full sequence of images is unwrapped, the last step – the reconstruction algorithm, is carried out. Its task is to combine a set of textures (such as those shown in figure 7R) into a map of the temperature distribution on the surface of the cylinder.

The algorithm assumes that the surface area seen by the camera is high enough for successive textures in sequence to overlap each other at their upper and lower parts (as illustrated in figure 5). These folds can be used in two ways, shown in figure 8.

**Direct connection:** for a series of textures of the same height, the heights of folds are equal. This allows to split the

folds in half their height and then connect the two neighboring textures.

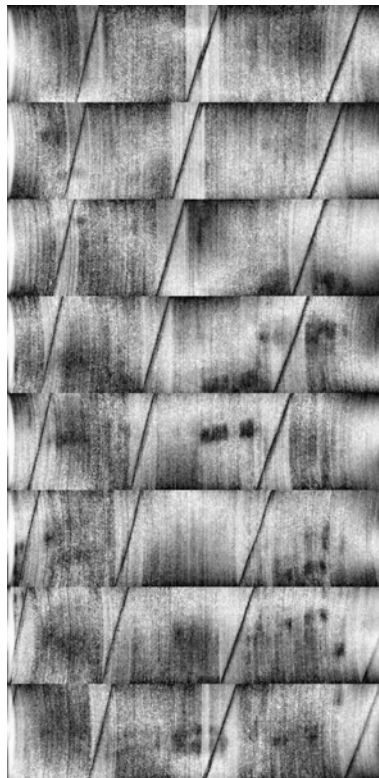


Fig.7R. Unwrapped and corrected textures

**Interpolated connection:** two textures can be connected by a fold which allows one texture to pass into the other. For this case, the algorithm uses a linear interpolation, guaranteeing a smooth transition between two consecutive textures. Interpolation is performed with a transfer function  $I_{coef}(i)$ , shown in figure 8 and used in the expression (6).

$$(6) M(i) = T_0(T_H - F_H + i)I_{coef}(i) + T_1(T_H - i)(1 - I_{coef}(i))$$

where:  $T_x(\bullet)$  – a row of texture  $x$ ,  $T_H$  - height of the texture,  $F_H$  - height of the fold.

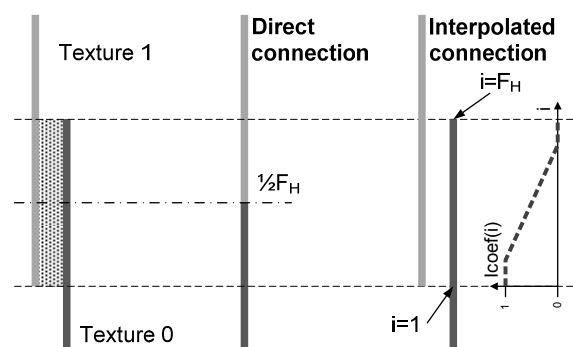


Fig.8. Two methods for consecutive textures connecting

One will notice that a direct connection is a trivial case of interpolated connection when the transfer function is built as a rapid transition from 1 to 0 at the  $\frac{1}{2}F_H$  point, in the middle of the fold.

The result of final reconstruction algorithm performed for the sample data from figure 7R was shown in figure 9 as a complete temperature distribution.

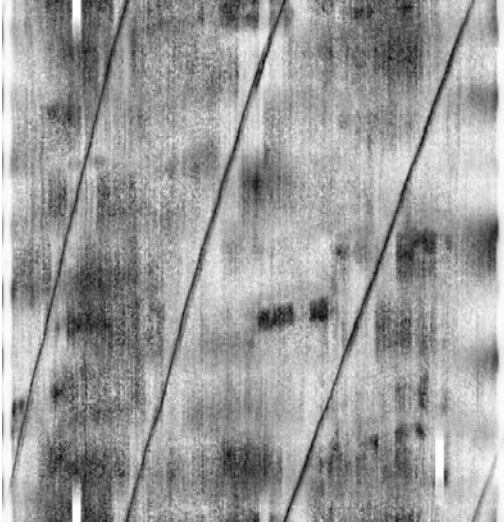


Fig.9. The final temperature distribution map of the rotating steel cylinder after surface reconstruction

### Results and discussion

The presented algorithm allows to process the measurement data stream, generated by a thermal IR camera, in such a way that a complete view of the temperature distribution of the rotating cylinder surface can be obtained.

Stream consists of momentary images of the object in different phases of its movement (in this case, a rotation).

The stream is divided into sequences with regard to communication errors and the use of synchronization pulses to determine the angular position of the individual image in the sequence is employed.

The sequence of  $N$  signed images is subject for processing which consists of eliminating the influence of the cylinder curvature, and then reconstructing a complete temperature distribution. Such generated temperature map can be used in the temperature control algorithms to regulate and sustain a desired profile of temperature on the surface of the cylinder. Also, it can be useful as a initial condition for numerical heating model of the object.

### Acknowledgments

This research was partially supported by a research project N N519 579838 from Polish National Science Centre.

### REFERENCES

- [1] Urbanek P., Model numeryczny zjawisk cieplnych w nagrzewanym indukcyjnie wirującym walcu, *Electrical Review*, (2007), nr 3, 71-74
- [2] [http://www.flir.com/uploadedFiles/Thermography\\_APAC/Products/Product\\_Literture/100930%20A615%20datasheet\\_en.pdf](http://www.flir.com/uploadedFiles/Thermography_APAC/Products/Product_Literture/100930%20A615%20datasheet_en.pdf) (checked on z 22/07/2012)
- [3] Cho C.-Y., Chen T.-M., Wang W.-S., Liu C.-N., Real-Time Photo Sensor Dead Pixel Detection for Embedded Devices Digital Image Computing, *International Conference on Techniques and Applications (DICTA)*, (2011), 164 -169
- [4] Jaworski T., Kucharski J., An Algorithm for Finding Visual Markers in an Infrared Camera Images Based On Fuzzy Spatial Relations, *Electrical Review*, (2012), this issue
- [5] Cyganek B., Komputerowe przetwarzanie obrazów trójwymiarowych, *Exit*, (2002)